Journal of Thermal Analysis, Vol. 49 (1997) 635-647

THE THERMAL BEHAVIOR OF TRIETHYLENEDIAMMONIUM SALTS
A combined investigation of $(trienH_2)[CoCl_4]$ and $(trienH_2)_2[(FeCl_4)_2(\mu\text{-}C_2O_4)]\cdot 2H_2O$ using TG–MS, FT–IR, and Raman spectroscopy[1]

M. Feist, R. Kunze**, D. Neubert**, K. Witke** and E. Kemnitz**

*Institut für Chemie der Humboldt-Universität zu Berlin, Hessische Straße 1-2, D-10115 Berlin

**Bundesanstalt für Materialforschung und -prüfung, Unter den Eichen 87, D-12205 Berlin, Germany

Abstract

$(trienH_2)[CoCl_4]$, which contains tetrahedral chlorocobaltate(II) anions, decomposes under argon in two stages via a stepwise deprotonation of the cation. The decomposition starts at 310°C with the liberation of HCl, followed at 400°C by the simultaneous release of a further mole of HCl and triene and/or its cracking products. The second decomposition stage is strongly influenced by the atmosphere. In the lower temperature region (<400°C), increasing oxygen contents of the carrier gas lead to decreasing mass losses. Therefore, the solid residues contain various amounts of C,N-containing products as well as coke. The thermal decomposition of the iron(III) compound, which contains μ-oxalato-bridged $FeCl_4$ units, begins with the dehydratation followed by the decay of the complex anion to produce CO, CO_2, and HCl. Instead of a binuclear, monooxobridged chloroferrate(III) complex, a $[FeCl_4]^-$ – containing compound is proposed as one of the final products. The third decomposition stage, partially overlaying the preceding one, is the degradation of the organic cation as found for the cobalt compound. The results of the *in situ*-TA–MS measurements are compared with those obtained from usual TA techniques as well as from the residue characterization by X-ray diffraction, Raman spectroscopy, and chemical analysis.

Keywords: bis-triethylenediammonium octachloro(μ-oxalato)diferrate(III) dihydrate, FT–IR- and Raman spectroscopy of triethylenediammonium salts, thermal behavior, TG–MS, triethylenediammonium tetrachlorocobaltate(II)

Introduction

Triethylenediammonium tetrachlorocobaltate(II), $(trienH_2)[CoCl_4]$, contains tetrahedrally coordinated anions, as recently found for the homologous 1,4-dimethylpiperazinium tetrahalogeno-metalates(II), $(dmpipzH_2)[M^{II}X_4]$ (M=Co, Zn;

1 Part V of: Halogenometalates of Transition Elements with Cations of N-heterocyclic Bases, Part IV: [1]

0368–4466/97/ $ 5.00

John Wiley & Sons Limited
Chichester

X=Cl, Br) [2, 3]. For such compounds, one should expect a thermal decomposition corresponding to their simple structure, i.e. the release of the base-HCl-adduct, leaving the metal halide behind:

$$(trienH_2)[CoCl_4] \rightarrow CoCl_2 + triene{\cdot}2HCl\uparrow$$

Recently, in the structure of $(trienH_2)_2[(FeCl_4)_2(\mu\text{-}C_2O_4)]\cdot 2H_2O$, we found a closely related anion, in which two tetrachloroferrate(III) units are μ-bridged by an oxalate group which results in the iron being octahedrally coordinated [4]. Therefore, a different decomposition mechanism had to be presumed. With regard to our investigations on the catalytic properties of solid halides and halometalates [5, 6], we found it interesting to compare the thermal behavior of the cobalt and the iron compound. It is known from literature that the thermal treatment of halometalate complexes containing nitrogenous heterocyclic bases or base cations may give product phases which reveal an enhanced catalytic activity. This effect has been attributed to channels or cavities that remain in the solid residues after the burning-out of the organic component. It is known and widely used in the chemistry of the aluminophosphate zeolites, the so-called ALPO's [7].

Experimental

All compounds have been measured by using a simultaneous thermal analyzer. The characteristic data (extrapolated onset temperature T_o, peak temperature T_p, mass loss Δm) have been obtained from the thermoanalytical curves (T, DTA, TG, DTG) by following the recommendations in [8]. Based on the thermoanalytical information, separate samples were tempered in dry argon or air, and were subsequently characterized by XRD, Raman spectroscopy, and chemical analysis (Table 1). In addition, *in situ*-TG–MS measurements have been carried out, which completed the interpretation of the decomposition steps.

Apparatus

The *s*imultaneous thermal analyzer Netzsch STA 429 was used with a mini sample carrier system with platinum crucibles and thermocouples Pt/PtRh10. α-Al_2O_3 was used as reference material. The carrier gas flow was 100 ml min^{-1}, Ar and air respectively. The heating rate β was 5 K min^{-1}, the sample mass 6–15 mg. Further the Seiko TG-DTA-220 was used connected with a mass spectrometer QMG 421 C (Balzers) via a heated stainless steel capillary (100°C). The gas flow was 200 ml He min^{-1}, β=10 K min^{-1}, sample mass 5–10 mg. The characteristic fragments have been measured in the multiple ion detection mode (MID) preceded by a measurement in the bargraph mode, in which a given interval of mass numbers (e.g. *m/e* 8...120) had been followed. For the completion of the analytical characterization the following measuring devices have been used: X-ray powder diffractometer HZG 4 (Freiberger Präzisionsmechanik); FT–IR spectrometer PE 2000 (Perkin Elmer) with TGS detector (resolution 4 cm^{-1}, 30 ml N_2 min^{-1}); Raman spectrometer Dilor XY with a Nitrogen-cooled CCD camera as detector (Argon laser Carl Zeiss ILA 120, excitation wave length 514 nm, laser power 1–6 mW on the sample).

Characteristic mass numbers

The interpretation of several frequently occurring lower mass numbers (e.g. 15, 17, 18, 28, 29) may turn out difficult. On one hand, they may be attributed to chemically different species (e.g. $N_2/CO/C_2H_4$ for 28 or $N_2H/COH/C_2H_5$ for 29). On the other hand, they are nearly omnipresent like nitrogen or water [9]. In our case, it had to be decided whether molecular nitrogen is formed during the complicated redox reactions or not. Therefore, the mass numbers m/e 28 and 29 ($^{14}N+^{14}N$ and $^{15}N+^{14}N$) have always been simultaneously followed even if other possible sources for *m/e* 15 (low natural abundance of ^{15}N) have to be taken into account. Generally, if the intensity-time curve is qualitatively identical for 28 and 29, then they are preferably attributed to N_2 and not to CO. On the other hand, the mass number 29 is practically always observed in the MS (similar to 15). In this case, one has to prove the non-formation of a given species via the continuous intensity decrease during the entire TG–MS measurement. The same is true for the mass numbers 17 and 18 being characteristic for water. Their intensities are often high, but this is primarily due to a greater ionization probability and is not a question of higher concentration. So here as well, the intensity decrease over the entire temperature interval is useful, and one should not misinterprete unexpectedly high intensity values for 17 and 18 as found for $(trienH_2)[CoCl_4]$ (Fig. 3a). The structure contains neither crystal water nor is it hygroscopic, nevertheless, the decay of the structure liberates considerable amounts of water because the compound has been prepared from an aqueous solution. Such a liberation of water from the 'depth of the grain' has been described for $K_2[SiF_6]$ [10] and further fluorides [11] , where a strong influence on the reaction behavior had been established. The mass number 15 practically always occurs in the MS if organic compounds are measured. It is formally attributed to methyl (CH_3) but is not typical because it is mostly formed via secondary protonation of methylene groups in the MS. As one may see (Figs 3, 6), this occurs even in the case of the triethylenediammonium compounds that do not contain methyl groups. Therefore, because the intensity curves for the mass numbers 15, 42, 55, 112 are parallel to each other, one concludes that their common source must be the triene molecule.

Synthesis

The title compounds were prepared as previously described [2, 4]; the hydrochlorides $(dmpipzH_2)Cl_2 \cdot H_2O$ and $(trienH_2)Cl_2$ were prepared by adding the free base to a hot 3*M* HCl, followed by filtration, crystallization at room temperature, and recrystallization from water. The products were washed with EtOH, air-dried, and chemically analyzed as described earlier [4].

Results and discussion

For the thermal decomposition of simple tetrachlorometalates like $(dmpipzH_2)[M^{II}Cl_4]$ (M=Co, Zn) under normal pressure one obtains TG curves

which are nearly unstructured. Therefore, they seem to confirm the expected simple one-step mechanism according to Eq. (1). The DTA traces, however, are unevaluable because they show multiple endothermal and exothermal effects overlaying each other (>285°C) which is obviously due to the degradation of the organic cation. Unexpectedly, changing to an oxidizing atmosphere does not simplify the decomposition behavior, and one obtains nearly identical DTA traces in air. Even if the mass loss in air (41.7%) differs from that obtained in argon (52.5%), the results cannot be interpreted in terms of a simple burning-out of the organic component leaving behind the metal oxide MO or the chloride MCl_2.

For $(trienH_2)[CoCl_4]$, however, a strong influence of the gas atmosphere on the decomposition had been established with as result that the thermoanalytical curves became much clearer (Figs 1, 2). Therefore, the thermal behavior of $(trienH_2)[CoCl_4]$ has been investigated in detail in order to compare it with the behavior of the iron complex.

$(trienH_2)[CoCl_4]$

First, the simple hydrochlorides $(dmpipzH_2)Cl_2 \cdot H_2O$[2] and $(trienH_2)Cl_2$[3] have been measured under argon. The TG step, which follows the endothermal effect of the solid state decomposition ($T_o \approx 200$°C), is endothermal as well because it represents the evaporation of the base-HCl adduct. The thermolysis of the organic base does not predominate, so that a mass loss of about 100% is observed. In the case of $(trienH_2)[CoCl_4]$, a more complicated situation is found. Summarizing the previously discussed results with the information obtained from the *in situ*-TA–MS and FT-IR measurements as well as from analytical data (Table 1), one concludes the following.

The thermal decomposition under normal pressure does not proceed via a liquid state. It is a two-step mechanism, which is best-expressed in pure argon. Here, one obtains two well separated endothermal effects at 311 and 398°C (Fig. 1, curve 1). The sum of the corresponding TG steps Δm_1 and Δm_2 in argon (Fig. 2) coincides well with the value calculated for the release of 'triene·2HCl' (58.78%). The TG–MS curves in Fig. 3a, b show that the first effect corresponds to the release of HCl (*m/e* 35, 36, 37, 38), whereas the second one is due to the simultaneous release of a further mole HCl and of triene and/or its cracking products (*m/e* 15, 42, 55, 112). So the deprotonation of the cation proceeds in a stepwise manner. At low temperatures of about 200°C, where the simple triethylenediammonium hydrochloride decomposes, the free, non-decomposed base triene is easily detected, and the attribution of the ion fragments [e.g. *m/e* 28, 42, 55, 56, 57, 84, 112(M^+)] is simple

2 Endo(I): T_o=80°C, T_p=115°C, Δm=9.1% (calcd. 8.78) [dehydratation]; Endo(II): T_o=199°C, T_p=202°C [decomposition], passing into Endo(III): T_o=252°C, T_p=273°C, $\Sigma\Delta m$=97.0% [product evaporation].

3 Endo(I): T_o=201°C, T_p=203°C, [solid state decomposition]; Endo(II)/Endo(III): T_o=251°C, T_p=295/327°C, Δm=96.4% [evaporation].

according to [12]. On the other hand, the decomposition of $(trienH_2)[CoCl_4]$ proceeds at considerably higher temperatures so that degradation predominates. Nevertheless, the free base may be detected, but only at much higher sensitivity of the MS (Fig. 3c, to compare with Fig. 6c!). The decomposition reactions that overlay the simple evaporation are complicated redox reactions of the organic cation. They give non-defined carbon and nitrogen containing products ($C_cH_hN_n$, cf. Table 1) which blacken the solid residues. In certain cases, even elementary carbon may be detected by Raman spectroscopy (ca. 1350, 1550 cm^{-1}).

This interpretation coincides well with the cited observation that the influence of the gas atmosphere on the thermoanalytical curves is qualitatively different in the first and the second decomposition stages. It is also clearly expressed in the TG traces (Fig. 2). Contrary to the first deprotonation of the base cation (Δm_1), that always proceeds at the same temperature, the second mass loss Δm_2 is shifted to lower temperatures with increasing amounts of oxygen. In the same way, increasing

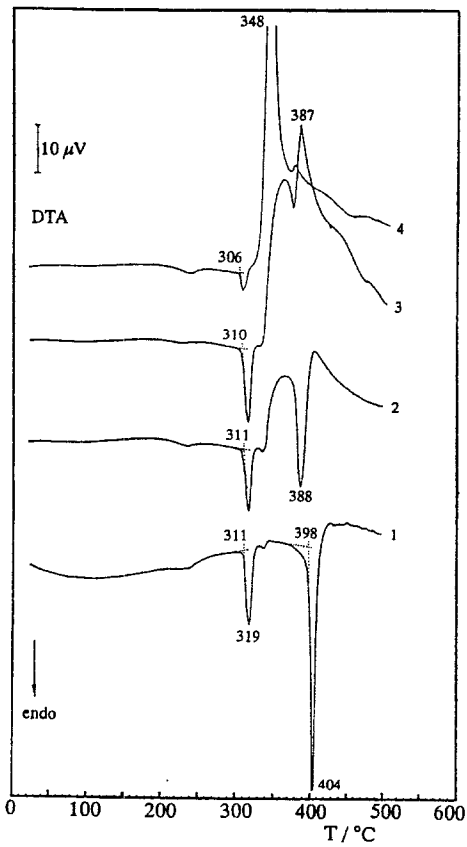

Fig. 1 DTA curves of $(trienH_2)[CoCl_4]$ in argon (1), and in air (4), and for increasing air contents in the carrier gas argon (2, 3). The curves 1-3 have been obtained after argon-flushing of the sample recipient for various times before starting the heating run: (1) 15 h; (2) 2 h; (3) 0.1 h

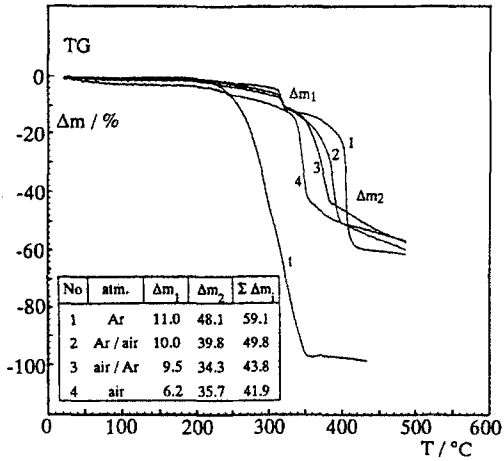

Fig. 2 TG curves of $(trienH_2)[CoCl_4]$ corresponding to the DTA curves in Fig. 1 compared with the TG curve of $(trienH_2)Cl_2$ (*t*)

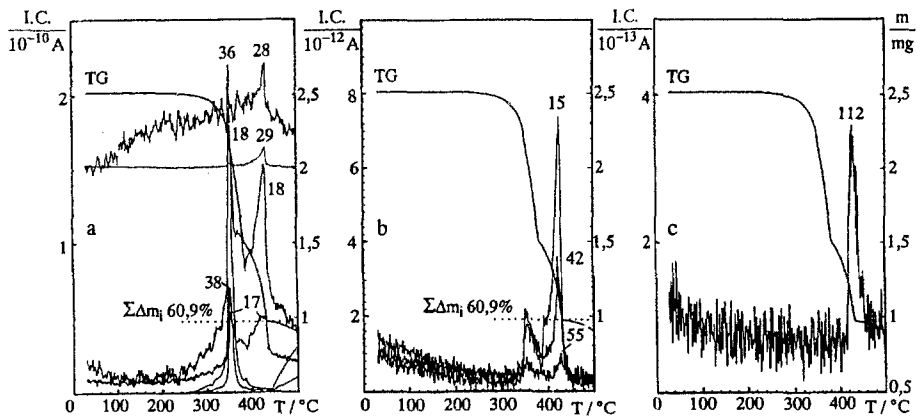

Fig. 3 TG–MS curves of $(trienH_2)[CoCl_4]$ in helium for different ion current sensitivities (The curves for *m/e* 28 and 29 have been shifted for a better legibility)

amounts of atmospheric oxygen in the carrier gas (up to normal air) result in a complete inversion of the heat exchange in the second part of the DTA curves above 330°C (Fig. 1). So the curves have to be understood as an overlay of the endothermal evaporation process by the exothermal decomposition reaction that becomes dominant with increasing amounts of air. In curve 2, where the carrier gas argon contains only very small amounts of oxygen, the endothermic effect is still distinctly observed, but is surrounded by the ascent flank and the slope of the exothermal signal. The latter becomes more dominant in curve 3 and, therefore, only a very small endothermal peak can be registered.

In good accordance with curve 4 in Fig. 2, which had been obtained using an independent measuring device, the TG–MS curves of $(trienH_2)[CoCl_4]$ in air

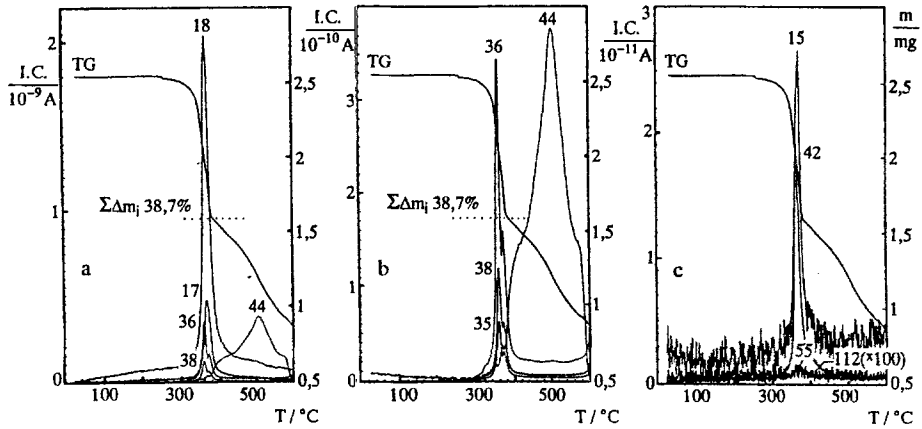

Fig. 4 TG–MS curves of (trienH_2)[$CoCl_4$] in air for different ion current sensitivities

(Fig. 4) indicate that the two step nature of the decomposition process practically disappears if the gas atmosphere is changed to an oxidizing one. Only a small subpeak may be distinguished for the liberation of HCl, and the carbon containing species are released at nearly the same temperatures. Furthermore, these TG–MS traces confirm the observation cited above that changing the atmosphere to an oxidizing one causes decreasing mass loss, which seemed to be contrary to usual chemical experience. Considerable amounts of carbon, nitrogen, and hydrogen actually remain in the solid residue after the main decomposition step and will be released at much higher temperatures as CO_2 (*m/e* 44). This is in good accordance with literature information [13] as with our previous results [14]. They actually prove that the decomposition of organic compounds in air in the temperature region below 400°C effects lower mass losses than in inert atmospheres. At higher temperatures, the situation is inverted and one observes the complete burning-out with the formation of CO_2, H_2O, N_2 and the expected greater mass losses.

The question of the formation of elementary nitrogen cannot be decided unequivocally. Normally, it does not occur in the case of tertiary amines. Nevertheless, it has been suspected, because primary investigations on the homologous compound (dmpipzH_2)[$CoCl_4$] also showed parallel intensity curves for the mass numbers 28 and 29. Furthermore, one could explain a possible nitrogen formation via the catalytic influence of the cobalt.

In the same way, FT–IR measurements seemed to favor the nitrogen formation by confirming the absence of further redox products like methane or ethylene (Fig. 5). So these compounds could not be interpreted in terms of another possible source for *m/e* 28 and 29. Contrary to literature information [12], we could show that both mass numbers have to be attributed to the fragmentation of the cation itself (i.e. C_2H_4 and C_2H_5 respectively), because they occur both in the mass spectrum of the free base triene and of the hydrochloride, and this with nearly the same maximal intensity.

Independent from this problem, the FT–IR shows impressively the separation of the main decomposition step into two partial processes. The spectra further confirm

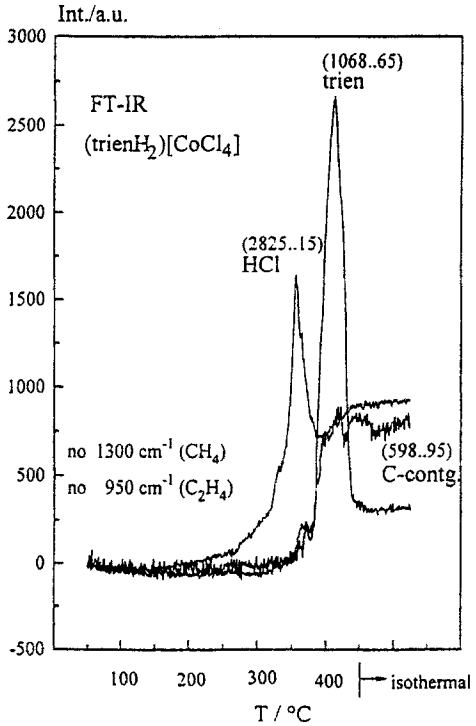

Fig. 5 FT–IR measurements on $(trienH_2)[CoCl_4]$ – Temperature dependence of the band intensity for characteristic wave numbers

the evaporation of the non-decomposed free base triene. The integral development of the band intensities during the entire measurement revealed that no other substances influence the IR spectrum. Scheme 2 summarizes the results obtained for $(trienH_2)[CoCl_4]$.

$(trienH_2)_2[(FeCl_4)_2(\mu\text{-}C_2O_4)]\cdot 2H_2O$

As it had to be expected, the structural differences between the μ-oxalato-bridged octachlorodiferrate and the simple chlorocobaltate complexes give rise to different decomposition behavior. Nevertheless, several similarities do exist, and the results which have been discussed before led to the understanding of the reactions of the iron complex. Figure 6 shows the TG–MS curves for different IC sensitivities.

The thermal decomposition begins with the release of both crystal water molecules in two TG steps near 100°C that overlay each other (calc. 4.82/found 5.3%). In the MS however, one observes only a broad, unstructured signal each for the mass numbers 17 and 18. Subsequently, the decay of the complex anion begins at 180°C with the release of CO and CO_2, which is easily derived from the structure of the anion. The decay proceeds via two strongly exothermal main steps (T_p 226,

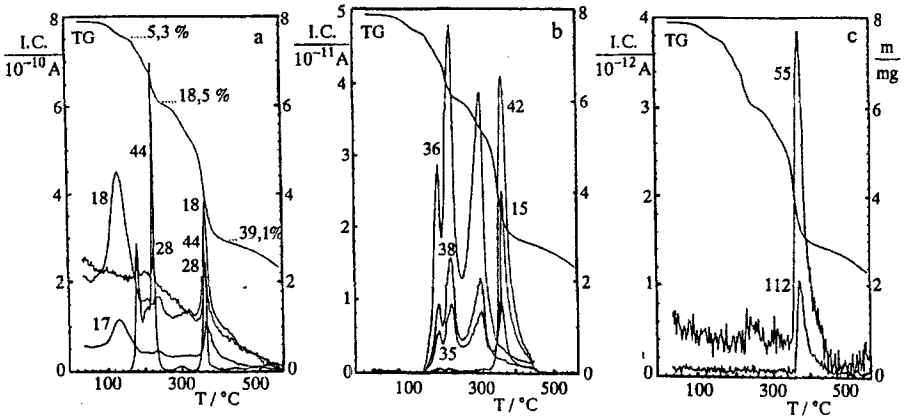

Fig. 6 TG–MS curves of $(trienH_2)_2[(FeCl_4)_2(\mu\text{-}C_2O_4)]\cdot 2H_2O$ in helium for different ion current sensitivities

354°C) whereby the second step is superposed by endothermal processes (T_p 375°C). The peak maxima in the DTG and the DTA curves coincide well with the intensity maxima for the mass numbers 28 for CO and 44 for CO_2 (Fig. 6a). Contrary to the case of $(trienH_2)[CoCl_4]$, here the attribution of the mass number 28 to CO is evident. And this is not only due to its simple derivation from the structure of the anion, but also due to a completely different intensity development of the mass numbers 28 and 29 (not shown in Fig. 6). A further difference in the behavior of the iron compound compared with that of $(trienH_2)[CoCl_4]$ is the early beginning of the HCl release (i.e. at nearly 180°C compared with 330°C). This may have two possible reasons which are closely related to each other.

Either in an early decomposition stage the simple hydrochloride is formed, which decomposes at about 200°C (cf. Fig. 2) and, therefore, could explain the release of HCl; or the decomposition of the anion itself produces HCl. In any case, this early appearence of HCl allows us to rule out two of the four possible mechanisms for the second decomposition step, i.e. the decay of the complex anion (Scheme 1). The reactions A and B are rejected for several reasons. Firstly, the found mass loss of nearly 18% considerably exceeds the values calculated for 2 moles CO_2 (11.77%) or for 2 moles CO (7.49%). Secondly, they would not explain the detection of HCl. Thirdly, the reactions A and B would not correspond to the simultaneous appearence of CO and CO_2. Furthermore, the chlorine balance for reaction A is incorrect and the formal charge of the hypothetical bis-oxo-bridged chloroferrate anion is too high (B).

On the other hand, the stability of the simple tetrachloroferrate anion is well-known (C), but in the same way there is literature information on the mono-oxo-bridged bidentate complexes as formed in reaction D. Finally, the Raman spectroscopic investigation of the intermediates[4] allowed us to favor the pathway C: The Raman spectrum of the product treated at 220°C (Fig. 7b) reveals the characteristic frequencies for $[FeCl_4]^-$ at 334 and 115 cm^{-1} [16, 17]. The absence of an intense

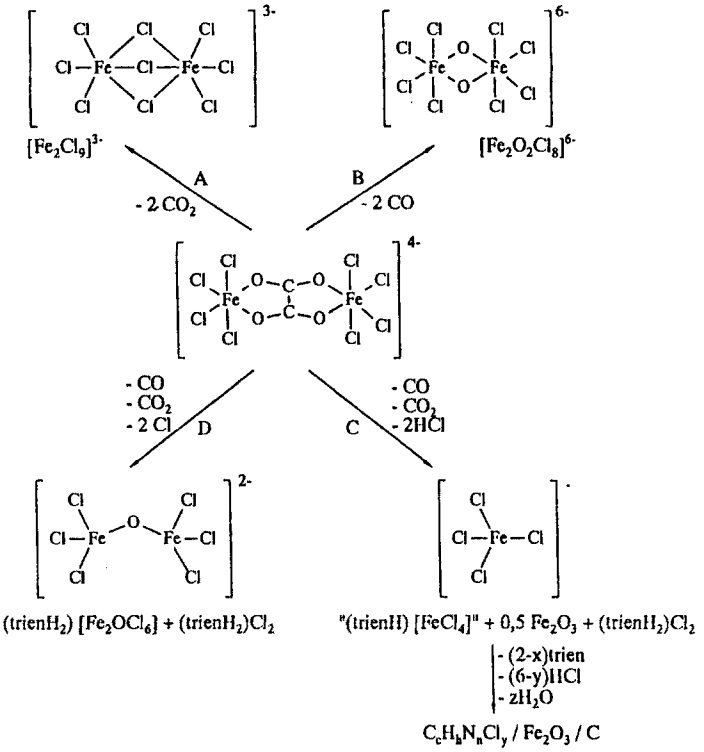

Scheme 1

Raman line at 188 cm^{-1} [18] proves the absence of $[Fe_2Cl_9]^{3-}$ in the product mixture[5]. Lastly, the chemical residue analysis also clearly suggests route C: Taking into account the HCl release and the formation of Fe_2O_3 in the solid at 220°C, the elemental ratio Fe/Cl in the residue must be 1:3, and not 1:4 as in the case of reaction D (Table 1).

HCl is released during the entire temperature interval after the dehydratation. As already found for $(trienH_2)[CoCl_4]$, the fragments of triene appear only in the last decomposition stage, but their concentration in the evolved gas is higher than it is observed for the cobalt complex. This is possibly due to the catalytical activity

4 Attribution of the Raman lines in the educt phase (Fig. 7a) by comparing with the spectrum of $(trienH_2)_2Cl_2$ and with literature data [19]: 802, 796, 604, 559, 400 (cation); 510 (νFe–$O_{oxalato}$); 320, 284, 240 (νFe–Cl).

5 In the spectra of the tempered samples one also observes weak Raman lines of the decomposed cations (796 cm^{-1}) as well as broad lines at 218, 280, 403 cm^{-1} being typical for α-Fe_2O_3 [20]. The spectrum for the dehydrated phase (120°C, not shown) is nearly identical with that of the educt. Three weak lines at 186, 275, 397 cm^{-1} additionaly appear and have been attributed to the dehydratation product because they disappear after tempering at higher temperatures.

Table 1 Mass loss, Δm, chemical residue composition [m-%], and XRD characterization of $(trienH_2)[CoCl_4]$ and $(trienH_2)_2[(FeCl_4)_2(\mu\text{-}C_2O_4)]\cdot 2H_2O$ treated in different atmospheres

	$(trienH_2)[CoCl_4]$							$(trienH_2)_2[(FeCl_4)_2(\mu\text{-}C_2O_4)]\cdot 2H_2O$			
	in Ar				in air			in Ar			
	calc.	250°C	270°C	380°C	250°C	270°C	380°C	calc.	120°C	220°C	400°C
Δm		0.4	0.9	46.5	0.3	0.7	39.8		4.7	17.2	32.9
C	22.88	22.5	22.7	19.2	22.7	22.8	20.5	22.48	23.5	23.5	21.0
H	4.49	5.0	4.4	1.9	4.0	3.8	2.5	4.32	4.1	4.4	2.9
N	8.90	8.9	9.0	2.4	9.1	9.1	6.2	7.49	7.7	9.0	8.7
Co/Fe	18.71	18.3	18.2	32.7	18.7	18.8	26.6	14.94	17.8	22.7	21.1
Cl	45.02	45.7	45.0	40.9	45.3	45.4	43.1	37.93	39.5	43.4	39.6
$n_M:n_{Cl}$	1:4.0	1:4.2	1:4.1	1:2.1	1:4.0	1:4.0	1:2.7	1:4	1:3.5	1:3.0	1:2.9
XRD		[1]	[1]	[2]	[1]	[1]	[2]		[3]	[4]	[5]

[1] educt phase, sometimes less-crystalline

[2] crystalline product, reflexes not fully attributed, traces $CoCl_2$, no Co, no CoO

[3] d-values and rel. intensities nearly identical with educt phase; dehydratation possibly topotactical

[4] amorphous

[5] partially crystalline, diffuse scattering background, α-Fe_2O_3

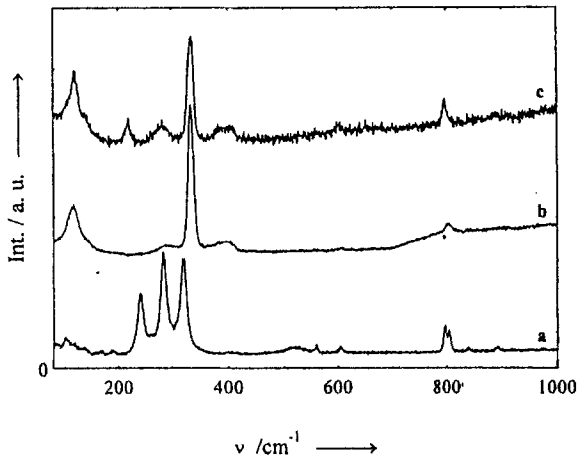

Fig. 7 Raman spectra of $(trienH_2)_2[(FeCl_4)_2(\mu\text{-}C_2O_4)]\cdot 2H_2O$ (a) and of samples tempered under argon: 220°C (b) and 400°C (c)

of cobalt. It is generally higher than the iron activity which might explain the higher degradation rate of the triene molecule in this case.

Figure 6a illustrates another interesting observation. The IC curves for the mass numbers 17 and 18 indicate that water is indeed released in the first decomposition step, is not released during the second stage, but is unexpectedly liberated in the third step once again. Thus, it has to be concluded that this water – contrary to the situation discussed before – is not an omnipresent inconvenience but rather has been formed secondarily in the complicated redox reactions during the decomposition of the organic cation. Because oxygen is already present in the iron compound, the formation of water can be easily explained. In summary, we obtain the decomposition scheme for $(trienH_2)_2[(FeCl_4)_2(\mu\text{-}C_2O_4)]\cdot 2H_2O$ presented in Scheme 2.

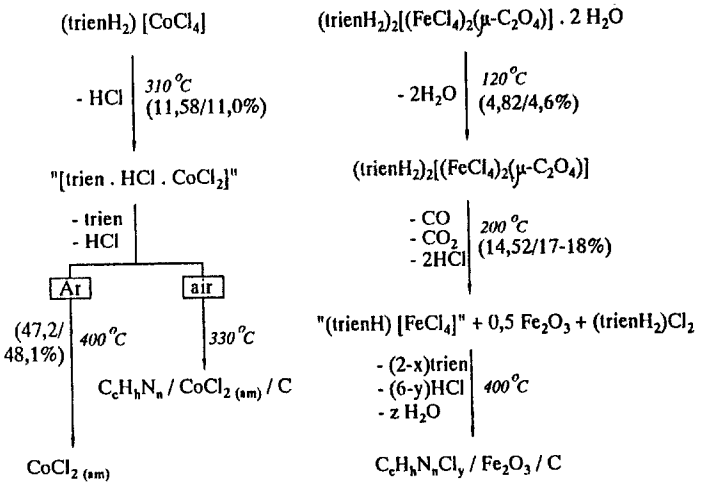

Scheme 2

The financial support by the Deutsche Forschungsgemeinschaft is gratefully acknowledged. The technical assistance of Margit Baumbach is gratefully acknowledged as well.

References

1 M. Feist, S. Trojanov and E. Kemnitz, Z. Naturforsch., 51b (1996) 1137.
2 M. Feist, S. Trojanov and E. Kemnitz, Z. Anorg. Allg. Chem., 621 (1995) 1775.
3 M. Feist, S. Trojanov and E. Kemnitz, Z. Naturforsch., 51b (1996) 9.
4 M. Feist, S. Trojanov and E. Kemnitz, Inorg. Chem., 35 (1996) 3067.
5 A. Heß, and E. Kemnitz, J. Catal., 149 (1994) 449.
6 E. Kemnitz and K.-U. Niedersen, J. Catal., 155 (1995) 283.
7 Heyong He, K. Alberti, T. L. Barr and J. Klinowski, J. Phys. Chem., 97 (1993) 13703.
8 G. Lombardi, For Better Thermal Analysis, Special Edn. of the Intern. Confederation for Thermal Analysis, University of Rome, 1980.
9 F. W. McLafferty and F. Turecek: Interpretation von Massenspektren, Spectrum Akademischer Verlag, Heidelberg, Berlin, Oxford 1995.
10 D.-H. Menz, W. Wilde and L. Kolditz, J. Fluorine Chem., 24 (1984) 345.
11 K. Heide, D.-H. Menz, C. Schmidt and L. Kolditz, Z. Anorg. Allg. Chem., 520 (1985) 32.
12 National Institute of Standards and Technology (NIST), USA, MS-Data Collection.
13 T. Hirata, T. Kashigawi and J. E. Brown, Macromolecules, 18 (1985) 1410.
14 R. Kunze and D. Neubert: TG–MS-Untersuchungen zum thermischen Abbau von Polymeren, Frühjahrstagung Polymerphysik Marburg, in: Verhandl. Dt. Phys. Ges., H.1, 1996, S.24.
15 M. G. B. Drew, V. McKee and S. M. Nelson, J. Chem. Soc. Dalton Trans., (1980) 80.
16 J. Shamir, B. J. Van der Keeken, M. A. Herman and R. Rafaeloff, J. Raman Spectr., 11 (1981) 215.
17 J. S. Avery, C. D. Burbridge and D. M. L. Goodgame, Spectrochim. Acta, 24A (1968) 1721.
18 K. Witke, K.-D. Schleinitz, M. Feist, D. Hass and M. Lorenz, Z. Anorg. Allg. Chem., 551 (1987) 215.
19 K. Nakamoto, Infrared and Raman Spectra of Inorganic and Coordination Compounds, Wiley & Sons, New York, Chichester, 3rd edn. 1978.
20 R. J. Thibeau, C. W. Brown and R. H. Heidersbach, Appl. Spectr., 32 (1978) 532.